

OPEN ACCESS

EDITED BY

Ying Luo,

University of Texas Southwestern Medical Center, United States

REVIEWED BY

Ling Niu,

Uniformed Services University of the Health

Sciences, United States

Shulin Mao, Harvard University, United States

*CORRESPONDENCE

Yurong Fu

sdsmuwito666@126.com

Zhengjun Yi

[†]These authors have contributed equally to this work and share first authorship

RECEIVED 05 July 2025 ACCEPTED 12 September 2025 PUBLISHED 08 October 2025

CITATION

Liu X, Wang W, Fu Y and Yi Z (2025) A novel circulating miRNA panel for early differential diagnosis of pulmonary tuberculosis from lung cancer with similar radiographic presentations.

Front. Med. 12:1660291. doi: 10.3389/fmed.2025.1660291

COPYRIGHT

© 2025 Liu, Wang, Fu and Yi. This is an open-access article distributed under the terms of the Creative Commons Attribution License (CC BY). The use, distribution or reproduction in other forums is permitted, provided the original author(s) and the copyright owner(s) are credited and that the original publication in this journal is cited, in accordance with accepted academic practice. No use, distribution or reproduction is permitted which does not comply with these terms.

A novel circulating miRNA panel for early differential diagnosis of pulmonary tuberculosis from lung cancer with similar radiographic presentations

Xiao Liu^{1,2†}, Wentao Wang^{1,2†}, Yurong Fu^{3*} and Zhengjun Yi^{1,2,4}*

¹School of Laboratory Medicine, Shandong Second Medical University, Weifang, China, ²Shandong Advanced Academy Engineering Research Institute for Precision Medicine Innovation and Transformation of Infectious Disease, Weifang, China, ³School of Basic Medical Sciences, Shandong Second Medical University, Weifang, China, ⁴Affiliated Hospital of Shandong Second Medical University, Weifang, China

This study aimed to establish a novel diagnostic approach based on a circulating microRNA (miRNA) panel to reliably distinguish pulmonary tuberculosis (PTB) from lung cancer (LC), particularly in patients presenting with overlapping radiographic features. A total of 592 participants were enrolled. In the discovery phase, miRNA expression profiles from 284 individuals, including PTB patients, LC patients, and healthy controls (HC), were analyzed to screen potential biomarkers. Candidate miRNAs were subsequently validated in an independent cohort of 308 plasma samples. The analysis revealed significant upregulation of hsa-miR-342-3p, hsamiR-199a-3p, and hsa-miR-199b-3p in PTB compared with LC. A diagnostic panel incorporating these three miRNAs demonstrated robust performance, achieving an area under the receiver operating characteristic curve (AUC) of 0.911 (95% confidence interval [CI]: 0.852-0.952) in the training set and 0.886 (95% CI: 0.780-0.953) in the validation set, with a sensitivity of 0.879. This miRNA panel outperformed the World Health Organization -endorsed Xpert MTB/RIF assay, effectively identifying early-stage PTB cases without cavity formation. These findings underscore the potential of miRNA-based diagnostics as a non-invasive and highly accurate tool for differentiating PTB from LC in patients with comparable imaging presentations, addressing a critical gap in pulmonary disease management.

KEYWORDS

miRNA, pulmonary tuberculosis, lung cancer, differential diagnosis, biomarker panel

Highlights

- Existing diagnostic approaches for PTB and lung cancer LC are limited by overlapping radiographic manifestations, reliance on invasive procedures, and suboptimal sensitivity.
- Plasma analysis revealed increased overexpression of hsa-miR-342-3p, hsa-miR-199a-3p, and hsa-miR-199b-3p in patients with PTB compared with those with LC.
- A diagnostic model incorporating these three miRNAs achieved high discriminatory power (training cohort AUC 0.911, validation cohort AUC 0.886), supporting its application for accurate, early, and non-invasive detection of PTB.

Introduction

Tuberculosis (TB) remains a pressing global health challenge and is still the leading cause of death from a single infectious agent. PTB, the most common clinical form, poses considerable diagnostic difficulties because its radiographic manifestations often overlap with those of LC. This similarity, combined with the limitations of existing non-invasive diagnostic techniques, usually leads to the misdiagnosis of PTB as LC (1–5). Accurate differentiation between PTB and LC, particularly in patients with comparable imaging features, is therefore crucial for timely treatment initiation and improved clinical outcomes.

Conventional non-invasive diagnostic methods, such as sputum smear microscopy and culture, are hampered by low sensitivity and long turnaround times. The Xpert MTB/RIF assay offers greater diagnostic accuracy; however, its high cost restricts its widespread use, especially in low-resource settings (6). Invasive procedures such as tissue biopsy can provide a definitive diagnosis but are not always accessible in resource-limited healthcare systems (7). These limitations underscore the urgent need for a rapid, reliable, and cost-effective non-invasive diagnostic strategy for PTB.

MicroRNAs, a class of small non-coding RNAs approximately 20–25 nucleotides in length, have emerged as highly stable biomarkers detectable in plasma and other body fluids, making them attractive candidates for non-invasive diagnostics (8, 9). Circulating miRNAs have shown diagnostic potential across multiple diseases, including malignancies and infectious conditions (10–12). Specific miRNAs are linked to the molecular pathogenesis of both LC and TB. For instance, hsa-miR-21–5p and hsa-miR-196b-5p have been implicated in the progression of LC, while hsa-miR-495 and hsa-miR-543 contribute to LC invasiveness (13–15). In TB, miRNAs such as hsa-miR-342, hsa-miR-222-3p, hsa-miR-431-3p, and hsa-miR-1303 play essential roles in regulating host innate immune responses (16, 17).

In this study, plasma miRNA profiles from 308 participants were analyzed, and a diagnostic classifier was developed using binary logistic regression to differentiate PTB from LC. The miRNA panel demonstrated higher sensitivity compared with conventional diagnostic methods, including Xpert MTB/RIF, sputum smear microscopy, and culture. These findings highlight the potential of miRNA–based assays as a precise, non-invasive strategy for improving early and accurate differentiation of PTB and LC.

Methods

Patient recruitment and sample collection

A total of 308 peripheral blood samples were collected from patients at Weifang No. 2 People's Hospital between March 2021 and March 2024. Blood was drawn into EDTA- K_2 anticoagulant tubes and centrifuged at 3000 rpm for 15 min at room temperature. The plasma fraction was then carefully separated and stored for subsequent RNA extraction. In addition to these clinical samples, miRNA expression profiles were obtained from publicly available datasets in the Gene Expression Omnibus (GEO) database, including GSE116542 1 , GSE31568, and GSE61741 (18, 19).

Reverse transcription-quantitative polymerase chain reaction

Total RNA was isolated from plasma samples using TRIzolTM LS Reagent (Thermo Fisher Scientific, Waltham, MA, United States) in accordance with the manufacturer's instructions. Complementary DNA (cDNA) was synthesized from the extracted RNA using the PrimeScriptTM II 1st Strand cDNA Synthesis Kit (Takara Bio, Shiga, Japan). Quantitative real-time PCR (qRT-PCR) was then conducted under the following thermal cycling conditions: initial denaturation at 95 °C for 30 s, followed by 40 amplification cycles consisting of denaturation at 95 °C for 5 s and annealing/extension at 60 °C for 30 s.

Primers specific for U6 small nuclear RNA (used as the endogenous control) and the three target miRNAs were synthesized by Sangon Biotech (Shanghai, China). Relative expression levels of miRNAs were calculated using the $2^{-\Delta Ct}$ method, where $\Delta Ct = Ct$ (miRNA) – Ct (U6).

The target miRNA sequences, sourced from the miRDB database, were as follows:

- hsa-miR-342-3p (23 bp): 5'-TCTCACACAGAAATCGCACC CGT-3'.
- hsa-miR-199a-3p (22 bp): 5'-ACAGTAGTCTGCACATTGG TTA-3'.
- hsa-miR-199b-3p (22 bp): 5'-ACAGTAGTCTGCACATTGG TTA-3'.

Verification against the GenBank database identified *Mus musculus* U6 small nuclear RNA-RnU6 (GeneID: 19862, 107 bp):

5'-GTGCTCGCTTCGGCAGCACATATACTAAAATTGGAAC GATACAGAGAAGATTAGCATGGCCCCTGCGCAAGGATGACA CGCAAATTCGTGAAGCGTTCCATATTTTT-3'.

Identification of candidate miRNA biomarkers

Differentially expressed miRNAs were identified using the GEO2R online analysis tool.² For the LC group, the selection threshold was set at $|\log_2 \text{ fold change (FC)}| \ge 0$, whereas for the PTB group, the threshold was $|\log_2 \text{FC}| \ge 1$ with a significance level of $p \le 0.05$. Here, FC represents the ratio of the mean gene expression level in patients compared with HC. To maximize the inclusion of potentially informative biomarkers, no false discovery rate (FDR) adjustment or other multiple-testing corrections were applied during the initial screening, and statistical significance was defined as $p \le 0.05$. Furthermore, candidate miRNAs were required to show opposing expression patterns between the PTB and LC groups to enhance their diagnostic relevance.

Diagnostic performance and clinical net benefit analysis

A binary logistic regression model was established using SPSS software, version 27.0.1 (IBM Corp., Armonk, NY, USA). The

¹ https://www.ncbi.nlm.nih.gov/geo/

² https://www.ncbi.nlm.nih.gov/geo/geo2r/

diagnostic performance of the model was assessed by generating receiver operating characteristic (ROC) curves and calculating the AUC with MedCalc Statistical Software, version 20.022 (MedCalc Software byba, Ostend, Belgium). Similarly, decision curve analysis (DCA) was conducted using R software, version 3.5.0 (R Development Core Team, Vienna, Austria), to evaluate the clinical net benefit of the predictive model.

Functional enrichment analysis of miRNA target mRNAs

Putative mRNA targets of the selected miRNAs were predicted using three publicly available databases: TargetScan version 7.2³, miRWalk⁴, and miRDB.⁵ Functional enrichment analyzes of the predicted target genes were then performed using Gene Ontology (GO) annotations and Kyoto Encyclopedia of Genes and Genomes (KEGG) pathway analysis via the Sangerbox online platform.⁶

Statistical analysis

An independent t-test was applied to evaluate differences between two groups, whereas one-way analysis of variance (ANOVA) was used for comparisons involving more than two groups. Sensitivity comparisons among diagnostic methods were performed according to the following criteria: when the sample size was $n \geq 40$ and all expected frequencies (T) were ≥ 5 , Pearson's chi-square test was used; when $n \geq 40$ with at least one expected frequency of $1 \leq T < 5$, the continuity-corrected chi-square test was applied; and when n < 40 or any expected frequency was T < 1, Fisher's exact test was employed. All statistical analyzes and graphical visualizations were conducted using GraphPad Prism software, version 8.0.2 (GraphPad Software, San Diego, CA, United States), and R software, version 3.5.0 (R Development Core Team, Vienna, Austria). A p-value of < 0.05 was considered statistically significant.

Results

Study participants and characteristics

A total of 308 participants were initially recruited for this study, comprising 128 patients with PTB, 109 patients with LC, and 71 HC. PTB cases were identified based on clinical symptoms and chest imaging findings consistent with tuberculosis. Among these, 86 patients were confirmed by positive results from *Mycobacterium tuberculosis* (MTB) culture, acid-fast bacilli (AFB) smear microscopy, the TB-LAMP assay, or the Xpert MTB/RIF test. The remaining 42 PTB cases were diagnosed based on clinical presentation, chest radiographic features, and a favorable response to anti-TB therapy, in accordance with the Chinese Clinical

Guideline for Diagnosis of PTB (WS 288-2017). LC cases were confirmed primarily through histological and/or cytological examination, supplemented by clinical evaluation when necessary. The HC group included individuals without respiratory symptoms and those with normal chest imaging results obtained within 3 months before enrollment. None of the participants had a history of PTB or other malignancies, and all were free from medical treatment within the 4 weeks preceding recruitment.

To minimize potential confounding, all participants were screened to exclude co-infections such as HIV and hepatitis B virus. Plasma samples that were hemolyzed or failed to meet RNA quality control criteria were excluded, resulting in 272 eligible samples for downstream analysis. The sample selection process is outlined in Figure 1, and the demographic and clinical characteristics of the 272 included participants are summarized in Table 1.

Identification of a 3-miRNA signature

The primary objective of this study was to identify a robust miRNA signature capable of distinguishing PTB from LC. In the current study, GEO datasets were analyzed, and 50 differentially expressed miRNAs were identified in a PTB dataset, along with 75 and 192 in two independent LC datasets. Comparative analysis revealed six overlapping candidates: hsa-miR-199a-3p, hsa-miR-199b-3p, hsa-miR-342-3p, hsa-miR-502-3p, hsa-miR-361-5p, and hsa-miR-423-5p. Because hsa-miR-502-3p, hsa-miR-361-5p, and hsa-miR-423-5p were consistently upregulated in both PTB and LC, they lacked discriminatory specificity and were excluded. Therefore, hsa-miR-342-3p, hsa-miR-199a-3p, and hsa-miR-199b-3p were selected as the candidate biomarker panel (Figure 2).

To establish a rapid, non-invasive diagnostic model, the plasma expression levels of these three miRNAs were quantified by RT-qPCR. Significant differences were observed in expression levels between PTB patients (n=77) and LC patients (n=68), as well as between PTB patients and healthy controls (HC, n=65) (Figure 3), supporting their potential clinical applicability.

Establishment and validation of a diagnostic model of the 3-miRNA panel

The diagnostic model was trained on the cohort using binary logistic regression analysis $[n=145\ (77\ PTB\ and\ 68\ LC)]$. The diagnostic score for each case was calculated using the following equation:

 $\frac{miRNA\;risk\;score = }{1 \over 1 + e^{-\left(-1.646 + 0.462 \cdot miR - 342 - 3p + 4.193 \cdot miR - 199a - 3p + 5.023 \cdot miR - 199b - 3p\right)}$

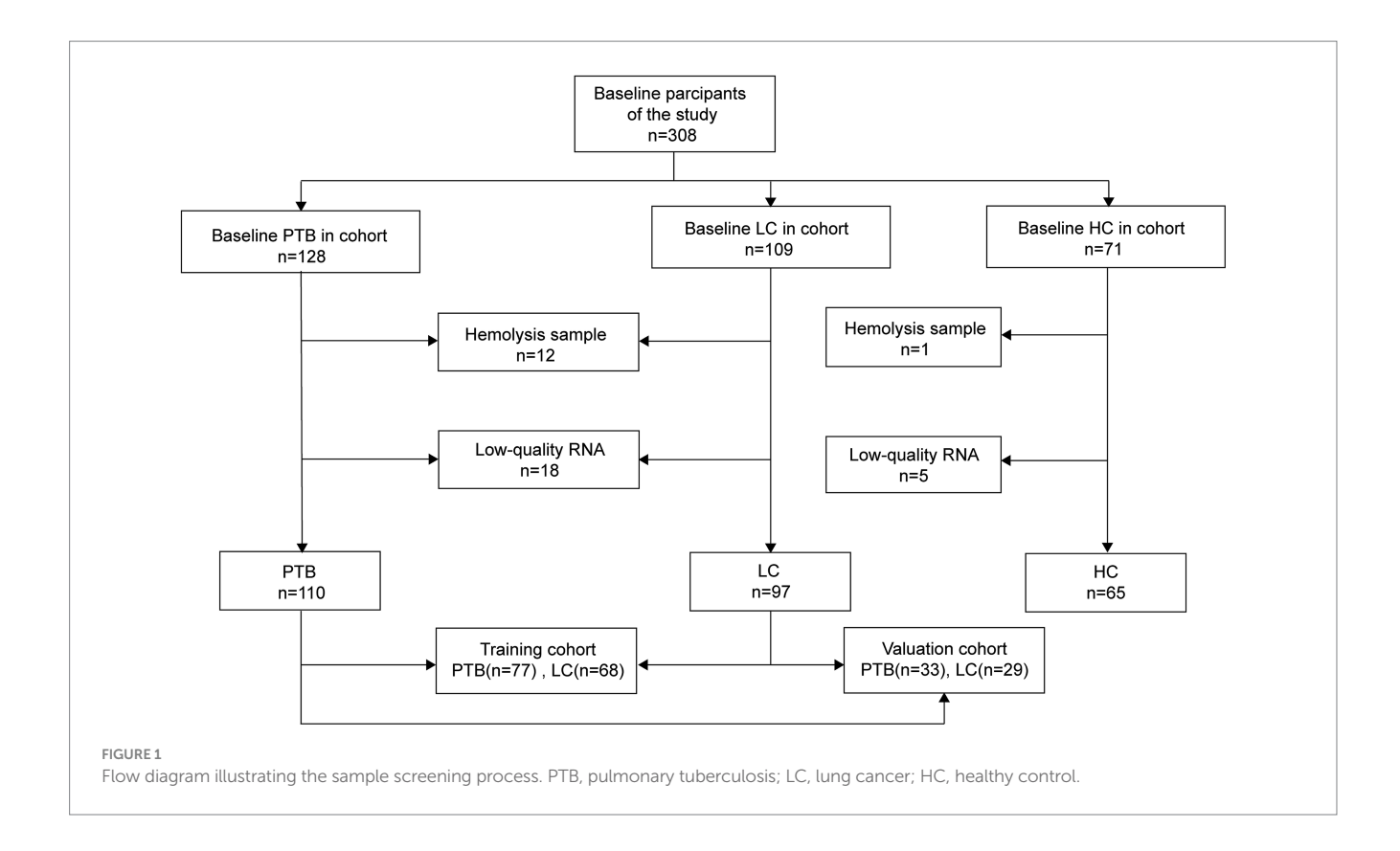
The diagnostic model demonstrated excellent performance in plasma samples from patients with PTB, yielding an AUC of 0.911 (95% CI: 0.852-0.952, p < 0.001; Figure 4A), with a sensitivity of 0.974 and a specificity of 0.765. Based on these findings from the training cohort, the model was further evaluated for robustness and accuracy in an independent validation cohort (n = 62; 33 patients with PTB and

³ https://www.targetscan.org/vert_72/

⁴ http://mirwalk.umm.uni-heidelberg.de/

⁵ http://www.mirdb.org/

⁶ http://sangerbox.com/



29 patients with LC). Validation testing confirmed the strong diagnostic application of the model, with an AUC of 0.886 (95% CI: 0.780-0.953, p < 0.001), a sensitivity of 0.879, and a specificity of 0.759 (Figure 4B).

For comparison, models constructed using only two miRNAs were also assessed; however, their AUC values were lower than those of the three-miRNA model, as summarized in Supplementary Table 1.

MiRNA panel: significant benefit in clinical practice

The clinical utility of any diagnostic tool depends on its ability to maximize accurate detection while minimizing the risks associated with misdiagnosis. In suspected LC cases, invasive procedures are often necessary, and both false-positive and false-negative results can lead to severe clinical consequences. To assess the practical applicability of the three-miRNA panel, DCA was performed (Figure 4C). In the test cohort, the DCA demonstrated that the miRNA panel consistently provided a higher net clinical benefit across all threshold probabilities compared with the default strategies of treating all patients or treating none. These results suggest that the panel may offer tangible clinical advantages by reducing the need for unnecessary invasive procedures and lowering the risk of diagnostic errors.

Age-related impact on miRNA expression and diagnostic performance

To examine the potential influence of age on miRNA expression and its implications for diagnostic accuracy, correlations between age and the expression levels of the three selected miRNAs were analyzed in patients with PTB. A negative correlation was observed, with expression levels decreasing as age increased (Figures 5A–C). The correlation coefficients were R = -0.45 (p = 0.008) for hsa-miR-342-3p, R = -0.45 (p = 0.009) for hsa-miR-199a-3p, and R = -0.48 (p = 0.005) for hsa-miR-199b-3p.

To further assess the effect of age on diagnostic performance, participants were stratified into two groups: younger (\leq 50 years) and older (\geq 51 years). The ROC curve analysis indicated improved diagnostic performance in the younger group, with an AUC of 0.950, compared with an AUC of 0.834 in the older group (Figures 5D,E). These results suggest that the diagnostic application of the miRNA panel may be particularly enhanced in younger individuals.

High sensitivity and early recognition in PTB compared to conventional methods

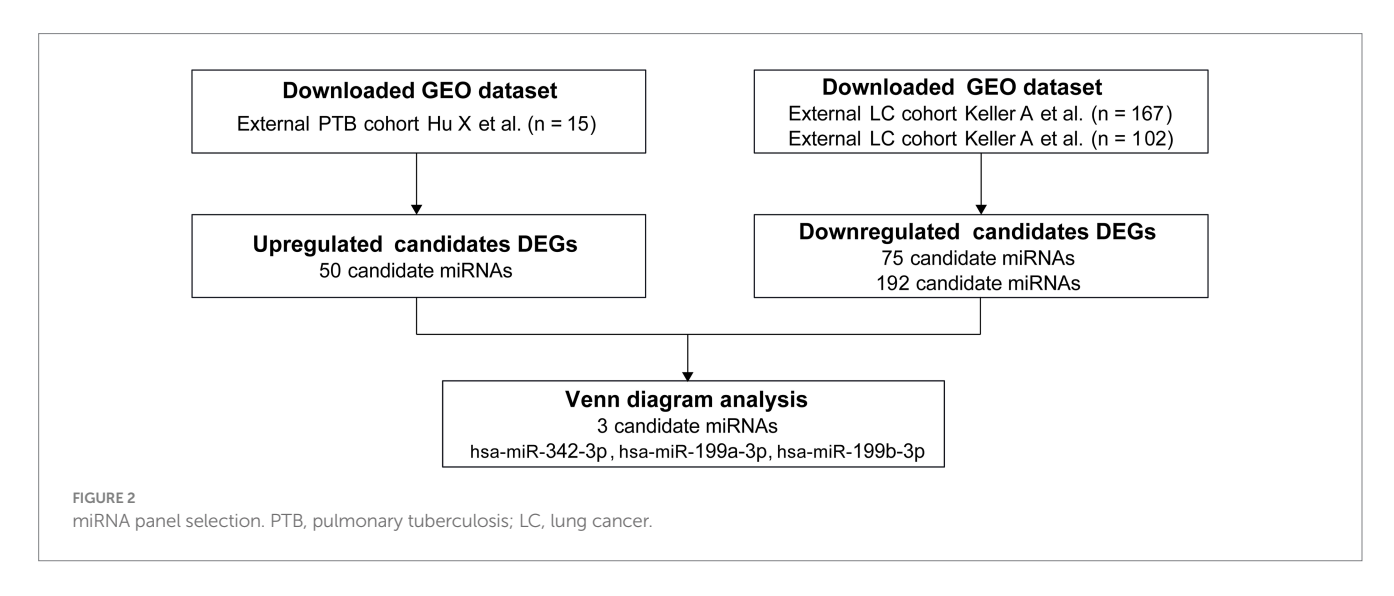
Early detection of PTB is critical for improving clinical outcomes. In the validation cohort, patients were initially stratified into early or late stages according to the presence or absence of pulmonary cavities. Recognizing that this single parameter has inherent limitations and may not adequately reflect the overall disease status, additional severity-related clinical indicators, including monocyte count, hemoglobin (Hb) levels, C-reactive protein (CRP), and erythrocyte sedimentation rate (ESR), were also evaluated to provide a more comprehensive assessment (20–24).

In PTB patients with cavitary disease, ESR, CRP, and monocyte counts were elevated compared with non-cavitary cases, whereas hemoglobin levels were significantly reduced (Figures 6A–E). These

TABLE 1 Characteristics of the study populations.

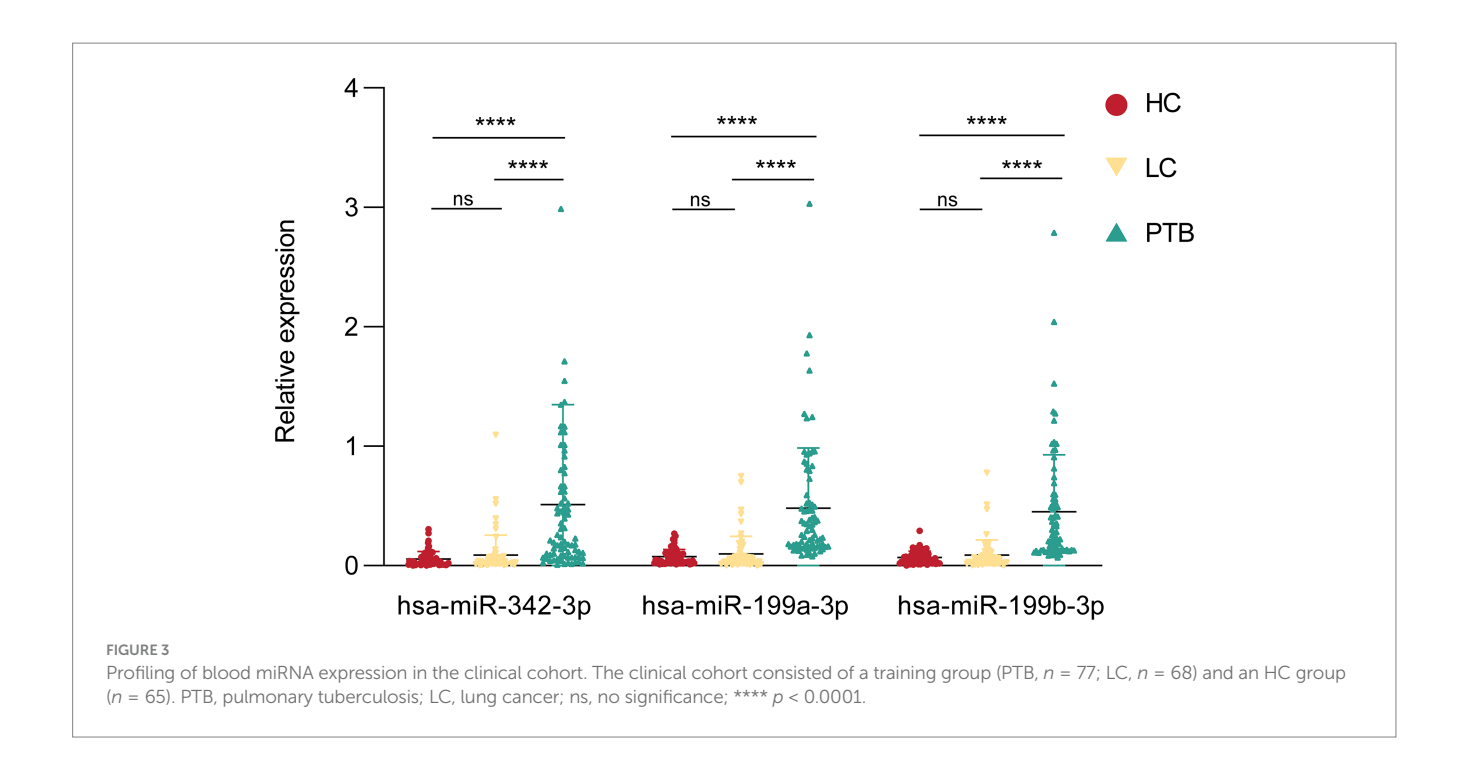
Characteristics	Category/Measure	Study population		
		PTB (n = 110)	LC (n = 97)	HC (n = 65)
Age at sampling	Mean±SEM	44.32 ± 1.82	61.18 ± 0.99	41.23 ± 2.12
Gender-counts	Male/Female	80/30	54/43	45/20
Clinical symptoms	Fever	21	3	0
	Fatigue and night sweats	4	1	0
	Cough	78	72	0
	Expectoration	67	66	0
	Haemoptysis	18	11	0
	Chest pain	10	13	0
	Asymptomatic	23	23	65
Presence of cavities	Positive	38	NA	NA
	Negative	72		
AFB smear	Positive	25	NA	NA
	Negative	60		
	NA	25		
TB-LAMP	Positive	39	NA	NA
	Negative	28		
	NA	43		
X-pert	Positive	58	NA	NA
	Negative	37		
	NA	15		
Culture	Positive	57	NA	NA
	Negative	42		
	NA	11		

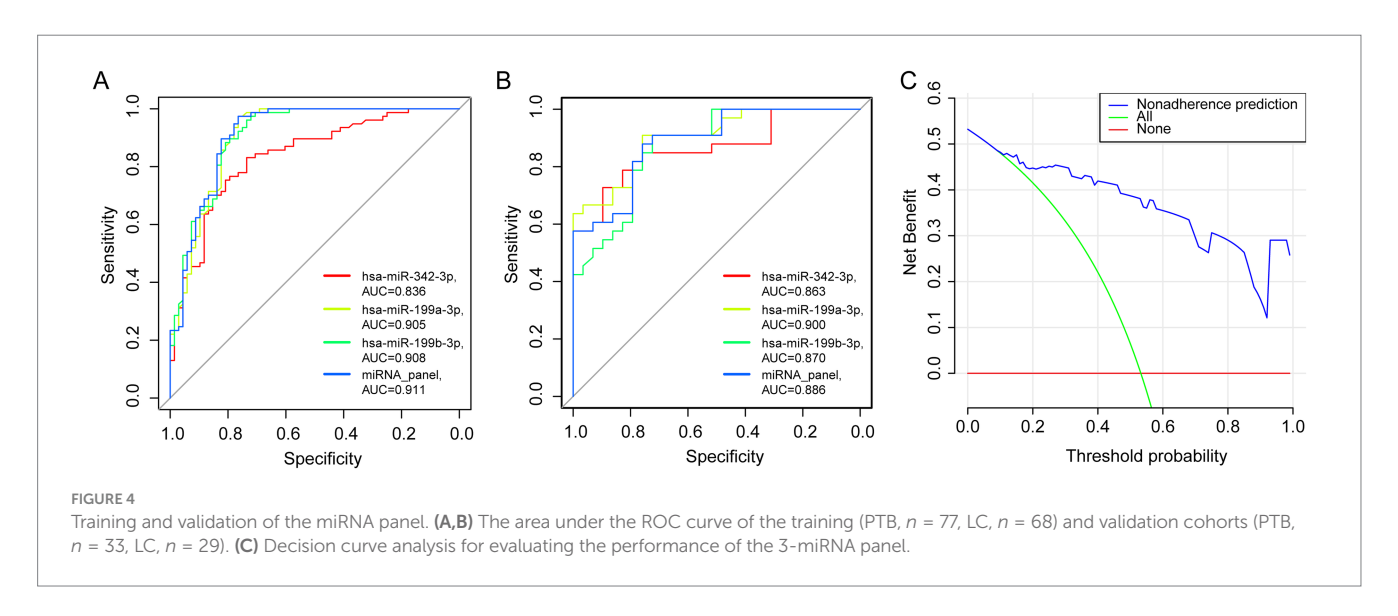
SEM, standard Error of Measurement; PTB, pulmonary tuberculosis; n, number; LC, lung cancer; HC, healthy control; SEM, Standard Error of the Mean; TB, tuberculosis; NA, not available; AFB, acid-fast bacteria.



results underscore apparent clinical differences between cavitary and non-cavitary stages of PTB. The diagnostic utility of the three-miRNA panel was then compared with conventional methods. Across PTB subgroups, the panel consistently demonstrated high sensitivity. In cavitary PTB, it significantly outperformed smear microscopy and

culture in detection sensitivity (p < 0.05). For non-cavitary PTB, the panel achieved sensitivity comparable to culture, although it did not surpass Xpert MTB/RIF (p < 0.05). When all PTB cases were assessed together, the miRNA panel showed higher sensitivity than Xpert MTB/RIF, smear microscopy, and culture (p < 0.05). These findings





suggest that the panel may serve as a viable diagnostic alternative in clinical practice, with performance matching or, in some cases, exceeding that of Xpert (Figure 6F).

Functional and pathway analysis of hsa-miR-342-3p and hsa-miR-199a/b-3p

To investigate the potential biological roles of the selected miRNAs in TB, GO enrichment analysis was conducted on their predicted target mRNAs. Target genes were identified based on the intersecting results from three prediction databases: TargetScan 7.2, miRWalk, and miRDB.

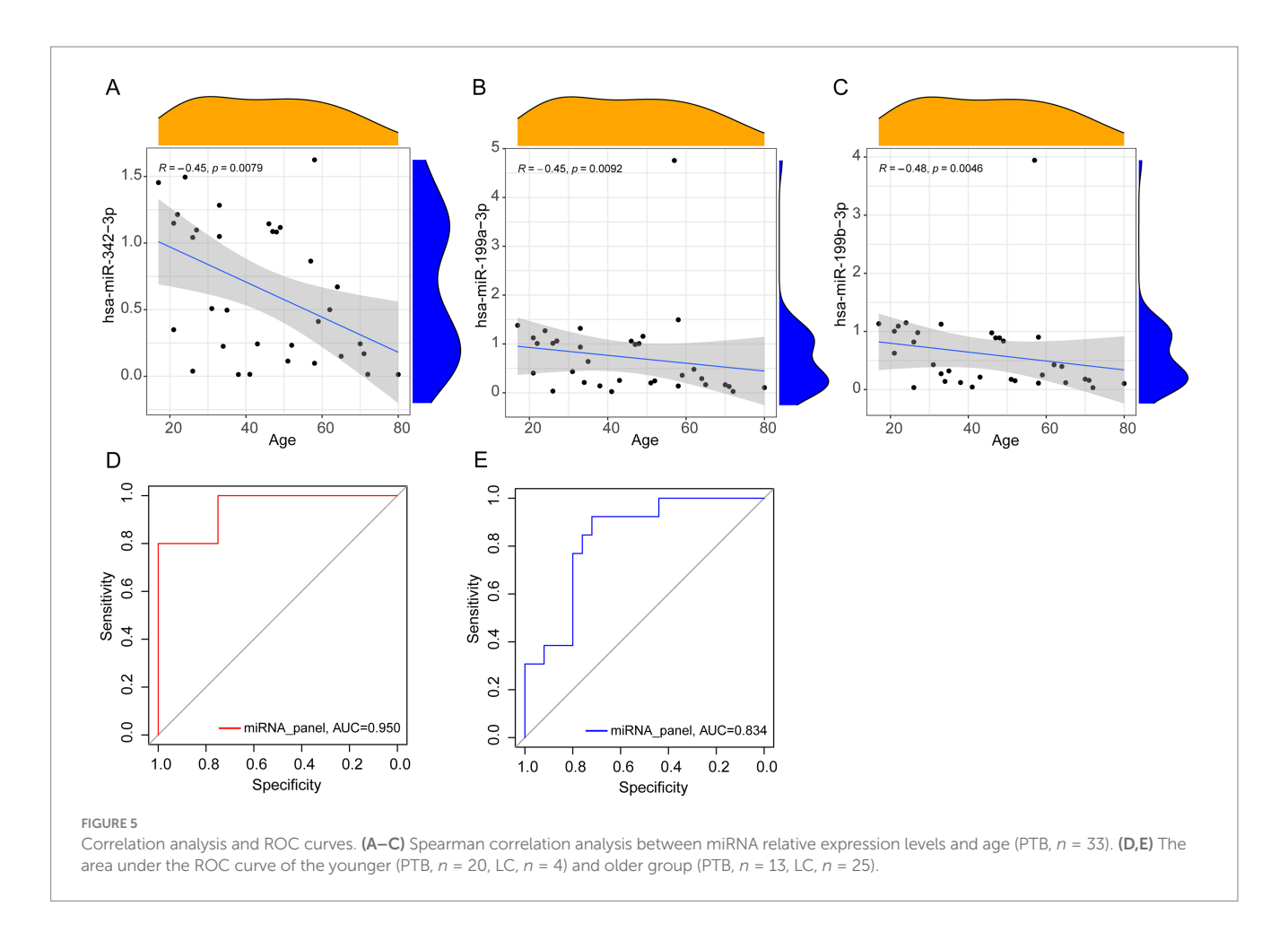
The GO analysis revealed that target genes of hsa-miR-342-3p were significantly enriched in biological processes, including positive regulation of gene expression, transcriptional regulation by RNA

polymerase II, and RNA metabolic regulation (Figure 7A). Similarly, target genes of hsa-miR-199a/b-3p were associated with pathways involved in positive regulation of gene expression, macromolecule metabolic processes, and overall metabolic regulation (Figure 7B).

Then, KEGG pathway enrichment analysis was performed to identify signaling pathways that these miRNAs may regulate. Genes targeted by hsa-miR-342-3p were mainly enriched in the Ras, TGF- β , and Jak–STAT signaling pathways (Figure 7C). However, target genes of hsa-miR-199a/b-3p showed significant enrichment in the PI3K-Akt, thyroid hormone, and sphingolipid signaling pathways (Figure 7D).

Discussion

In clinical practice, distinguishing PTB from LC in patients with overlapping radiological presentations remains a significant challenge,

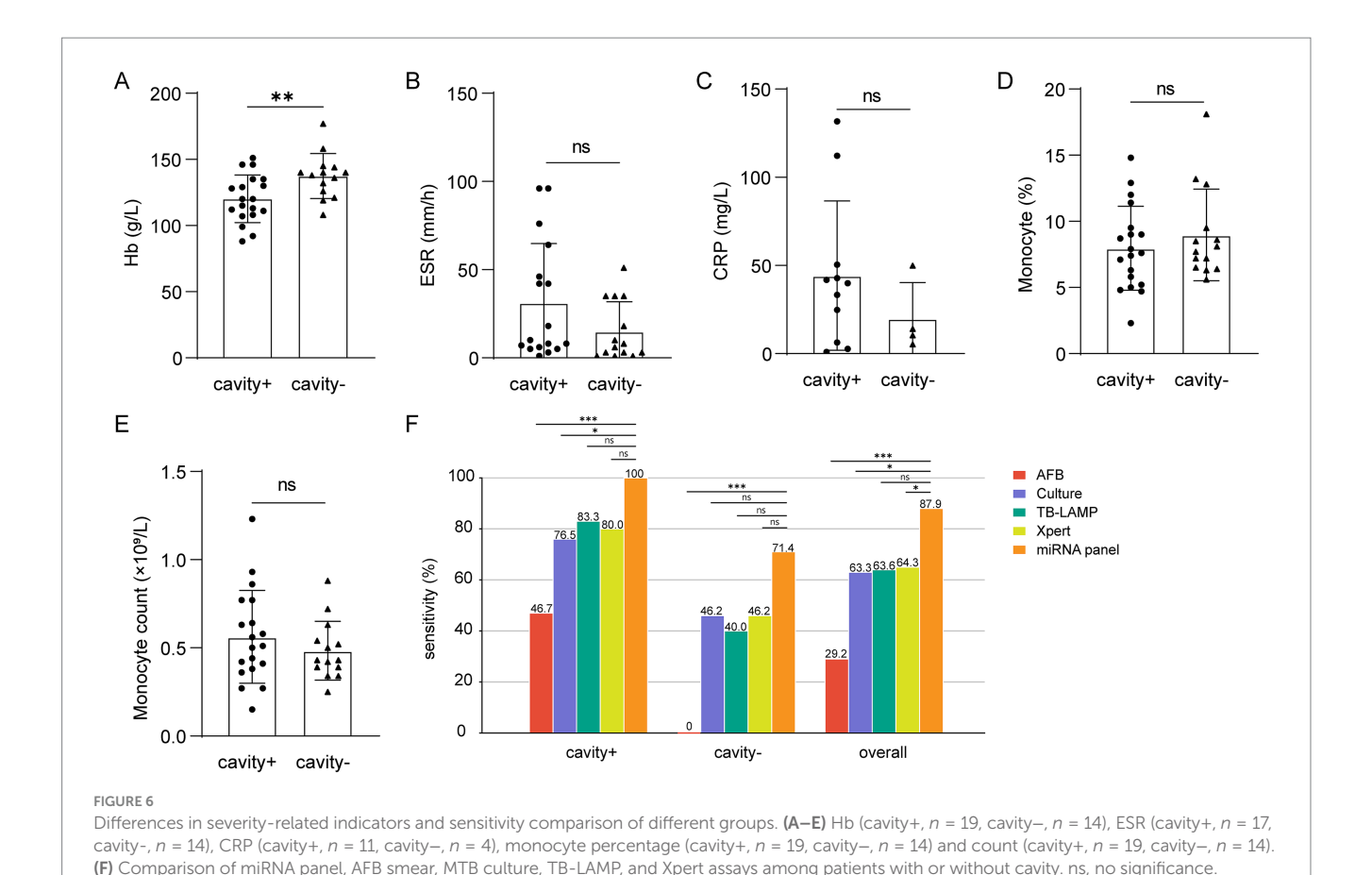


as conventional non-invasive diagnostic methods are often limited by prolonged turnaround times and insufficient sensitivity. An effective diagnostic tool should ideally be rapid, affordable, and non-invasive, enabling the timely and accurate differentiation of conditions. Addressing the limitations of current strategies necessitates the development of innovative approaches that improve diagnostic precision. Although recent efforts in non-invasive rapid detection have primarily concentrated on advancements in radiological techniques (25), their diagnostic accuracy remains inadequate and requires further refinement.

In this context, molecular biomarker-based detection strategies are gaining increasing attention as a promising alternative. Extensive evidence suggests that miRNAs play a crucial role as key regulators in both infectious immune responses and tumor progression. The biological functions of the miRNA panel identified in this study are closely aligned with these pathological processes. For instance, the predicted target genes of hsa-miR-342-3p are highly enriched in pathways regulating gene expression, particularly the TGF- β and JAK-STAT signaling cascades, which is consistent with its established roles in tuberculosis and cancer biology. In PTB, hsa-miR-342-3p enhances host defense by targeting SOCS6, a negative regulator of the JAK-STAT pathway, promoting the secretion of pro-inflammatory cytokines and inducing macrophage apoptosis (16, 26). It's observed that upregulation in PTB may therefore represent a host-protective response. By contrast, in NSCLC and other solid tumors, hsa-miR-342-3p functions as a tumor suppressor, inhibiting oncogenic drivers such as AGR2 and FOXQ1, while its association with the TGF- β pathway suggests a role in modulating the tumor microenvironment (27, 28). The frequent downregulation of hsa-miR-342-3p in cancer is likely attributable to the immunosuppressive conditions of the tumor microenvironment, which attenuate its tumor-suppressive activity.

Members of the hsa-miR-199 family (hsa-miR-199a-3p and hsa-miR-199b-3p) display enrichment in metabolic regulation and cancer-associated pathways. In models of septic acute kidney injury, these miRNAs modulate cellular homeostasis by suppressing Nrf2-mediated antioxidant gene expression (29, 30). Given the elevated oxidative stress associated with TB infection, this mechanism may contribute to the pathophysiology of PTB. The upregulation of hsa-miR-199a/b-3p in PTB serum likely reflects a compensatory host response aimed at curbing excessive inflammation while maintaining Nrf2-dependent antioxidant defenses. In NSCLC, the hsa-miR-199 family acts as a tumor suppressor primarily by inhibiting the Rheb-mTOR axis, a central pathway governing metabolic homeostasis and biosynthesis (31). Its downregulation in cancer may similarly result from the immunosuppressive tumor microenvironment, which impairs tumor-suppressive signaling.

The miRNA panel assessed in this study demonstrated robust diagnostic accuracy for distinguishing PTB from LC across both training and validation cohorts, with sensitivity and specificity



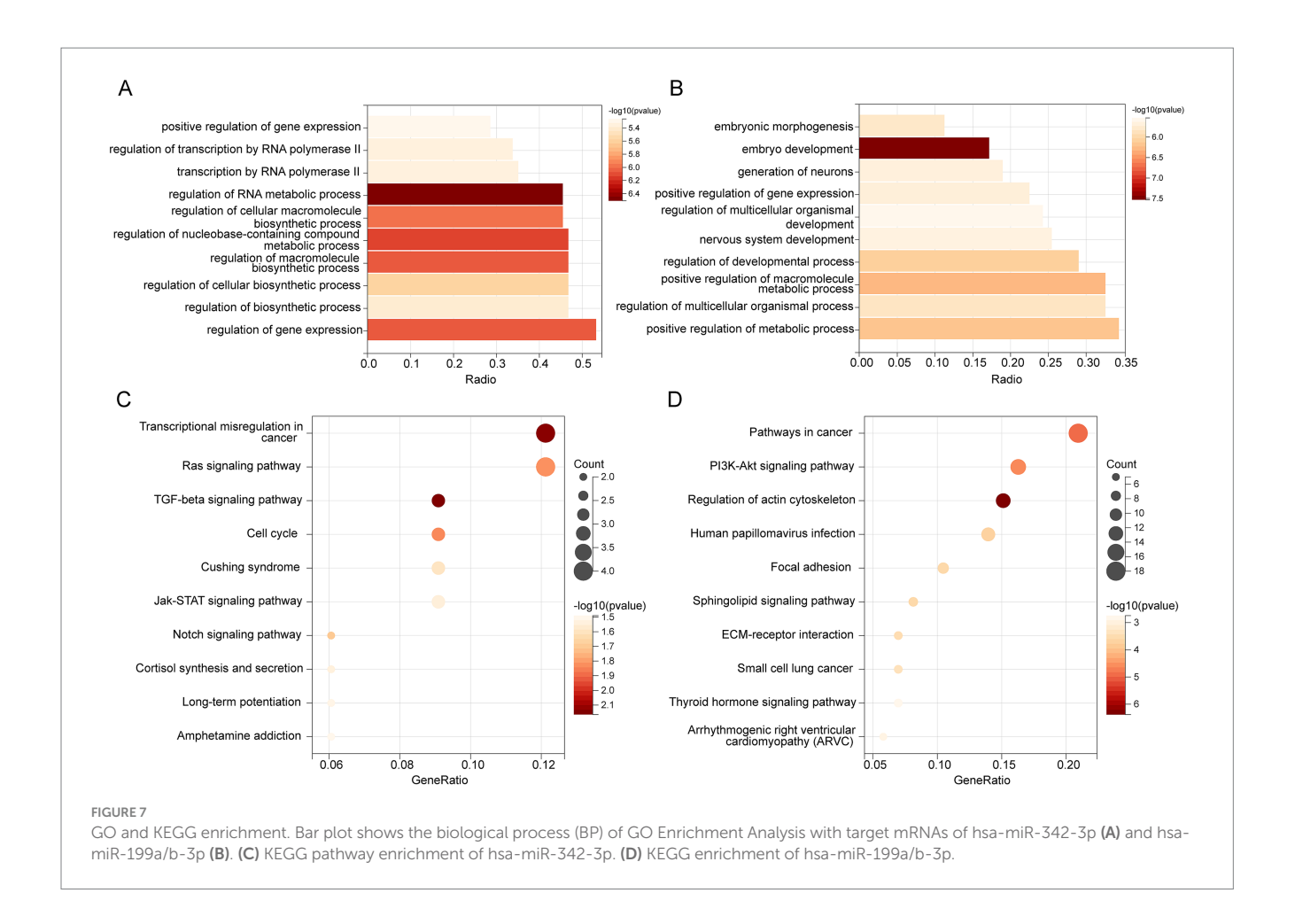
comparable to, and in some instances superior to, those of several commonly used biomarkers. In comparison with cell-free DNA (cfDNA)-based detection methods, the panel showed higher sensitivity, largely because cfDNA released from tuberculous necrotic foci often overlaps with tumor-derived cfDNA, reducing the discriminative value of quantitative cfDNA analysis (32). Regarding circular RNAs (circRNAs), their application in differential diagnosis remains mainly exploratory. Currently, no reliable circRNA markers with stable and consistently opposite expression patterns between PTB and LC have been identified. Furthermore, the complexity and high cost of circRNA detection further limit their clinical applicability at the primary care level (33). Furthermore, when compared with combined tumor marker detection, miRNA expression offers distinct advantages, as it is less influenced by inflammation and demonstrates greater stability and reproducibility in clinical samples (34). These attributes underscore the superior overall performance and translational potential of the identified miRNA panel.

* p < 0.05. ** p < 0.01. *** p < 0.001.

Beyond these comparisons, the panel's sensitivity for early PTB detection was further evaluated against conventional diagnostic methods, including culture, Xpert assay, AFB smear microscopy, and LAMP, in clinical settings. For this purpose, patients without pulmonary cavities were classified as having early-stage PTB, while those with cavities were considered to have late-stage PTB. Across both stages, the panel demonstrated diagnostic performance comparable to, and in some cases exceeding, that of Xpert, particularly in early disease detection, where reliable differentiation is most critical.

Although Xpert remains a widely validated diagnostic platform, our results suggest that the proposed approach could serve as a valuable complementary tool, particularly in resourceconstrained settings or in scenarios where rapid diagnosis is critical. Numerous studies have confirmed the remarkable stability of miRNAs under diverse storage conditions: they can remain preserved for more than 17 years at -80 °C, remain stable for up to 7 days at 4 °C, and exhibit no significant degradation for at least 24 h at room temperature. These characteristics fulfill the stringent criteria required for reliable clinical diagnostics (35, 36). In the present study, all plasma samples were either processed for immediate miRNA extraction or subjected to a single freeze-thaw cycle at -80 °C within 1 hour of collection. Further, stringent quality control procedures were implemented throughout all pre-analytical stages to minimize technical variation, ensuring both analytical precision and reproducibility.

However, several limitations of this study should be acknowledged. First, patients with concurrent PTB and LC were excluded due to the rarity of such cases; as a result, miRNA expression patterns in this subgroup were not evaluated. Second, since LC patients do not typically undergo TB-specific diagnostic testing, direct comparisons of TB detection specificity across different diagnostic methods could not be performed. Moreover, although efforts were made to minimize confounding factors during sample selection, such as excluding individuals with co-infections, other variables, including concurrent infections and age-related differences, may still influence the diagnostic accuracy of the miRNA panel in real-world clinical settings.



To address these gaps, future studies should expand cohort sizes and incorporate more diverse patient populations, while also benchmarking the panel against emerging state-of-the-art diagnostic technologies. Such investigations will be essential to further validate and refine the clinical translational potential of this miRNA-based diagnostic strategy.

Conclusion

In summary, this study established a rapid and non-invasive diagnostic strategy capable of differentiating PTB from LC in patients with overlapping radiological presentations. The identified miRNA panel demonstrated higher sensitivity compared to conventional methods, including Xpert MTB/RIF, smear microscopy, and culture, while also offering a lower cost and greater feasibility. These attributes highlight its strong potential for clinical translation, particularly in resource-limited settings, where it may serve as a practical and effective tool for diagnosing focal pulmonary lesions.

Data availability statement

The raw data supporting the conclusions of this article will be made available by the authors, without undue reservation.

Ethics statement

The studies involving humans were approved by Shandong Second Medical University Medical Ethics Committee. The studies were conducted in accordance with the local legislation and institutional requirements. The participants provided their written informed consent to participate in this study.

Author contributions

XL: Methodology, Supervision, Writing – review & editing. WW: Writing – original draft, Writing – review & editing. YF: Writing – review & editing. ZY: Validation, Writing – original draft, Writing – review & editing.

Funding

The author(s) declare that financial support was received for the research and/or publication of this article. This work was supported by a grant from the Natural Science Foundation of Shandong Province (No. ZR2021MH401).

Acknowledgments

We sincerely appreciate the financial support provided by the Program of Shandong Province Natural Science Foundation of China (No. ZR2021MH401). We thank all participants who agreed to take part in this study, and the Weifang NO.2 People's Hospital who assisted in patient consultation and sample collection.

Conflict of interest

The authors declare that the research was conducted in the absence of any commercial or financial relationships that could be construed as a potential conflict of interest.

Generative AI statement

The authors declare that no Gen AI was used in the creation of this manuscript.

References

- 1. Kim H, Kim HY, Goo JM, Kim Y. Lung Cancer CT screening and lung-RADS in a tuberculosis-endemic country: the Korean lung Cancer screening project (K-LUCAS). *Radiology.* (2020) 296:181–8. doi: 10.1148/radiol.2020192283
- 2. Saleemi SA, Alothman B, Alamer M, Alsayari S, Almogbel A, Mohammed S. Tuberculosis presenting as metastatic lung cancer. *Int J Mycobacteriol*. (2021) 10:327–9. doi: 10.4103/ijmy.ijmy_89_21
- 3. Niyonkuru A, Chen X, Bakari KH, Wimalarathne DN, Bouhari A, Arnous MMR, et al. Evaluation of the diagnostic efficacy of 18F-Fluorine-2-deoxy-D-glucose PET/CT for lung cancer and pulmonary tuberculosis in a tuberculosis-endemic country. *Cancer Med.* (2020) 9:931–42. doi: 10.1002/cam4.2770
- 4. Lang S, Sun J, Wang X, Xiao Y, Wang J, Zhang M, et al. Asymptomatic pulmonary tuberculosis mimicking lung cancer on imaging: a retrospective study. *Exp Ther Med.* (2017) 14:2180–8. doi: 10.3892/etm.2017.4737
- 5. Shu CC, Chang SC, Lai YC, Chang CY, Wei YF, Chen CY. Factors for the early revision of misdiagnosed tuberculosis to lung Cancer: a Multicenter study in a tuberculosis-prevalent area. *J Clin Med.* (2019) 8:700. doi: 10.3390/jcm8050700
- Steingart KR, Schiller I, Horne DJ, Pai M, Boehme CC, Dendukuri N. Xpert[®] MTB/ RIF assay for pulmonary tuberculosis and rifampicin resistance in adults. *Cochrane Database Syst Rev.* (2014) 2014:CD009593. doi: 10.1002/14651858.CD009593.pub3
- 7. Prabhakar B, Shende P, Augustine S. Current trends and emerging diagnostic techniques for lung cancer. *Biomed Pharmacother*. (2018) 106:1586–99. doi: 10.1016/j.biopha.2018.07.145
- 8. Balzano F, Deiana M, Dei Giudici S, Oggiano A, Baralla A, Pasella S, et al. miRNA stability in frozen plasma samples. *Molecules*. (2015) 20:19030–40. doi: 10.3390/molecules201019030
- 9. Ward Gahlawat A, Lenhardt J, Witte T, Keitel D, Kaufhold A, Maass KK, et al. Evaluation of storage tubes for combined analysis of circulating nucleic acids in liquid biopsies. *Int J Mol Sci.* (2019) 20:704. doi: 10.3390/ijms20030704
- 10. Dar GM, Agarwal S, Kumar A, Nimisha, Apurva, Sharma AK, et al. A non-invasive miRNA-based approach in early diagnosis and therapeutics of oral cancer. *Crit Rev Oncol Hematol.* (2022) 180:103850. doi: 10.1016/j.critrevonc.2022. 103850
- 11. Gahlawat AW, Witte T, Haarhuis L, Schott S. A novel circulating miRNA panel for non-invasive ovarian cancer diagnosis and prognosis. *Br J Cancer.* (2022) 127:1550–6. doi: 10.1038/s41416-022-01925-0
- 12. Lee JS, Kim S, Kim S, Ahn K, Min DH. Fluorometric viral miRNA Nanosensor for diagnosis of productive (lytic) human cytomegalovirus infection in living cells. *ACS Sens.* (2021) 6:815–22. doi: 10.1021/acssensors.0c01843
- 13. Zhou Y, Zhang Y, Xu J, Wang Y, Yang Y, Wang W, et al. Schwann cell-derived exosomes promote lung cancer progression via miRNA-21-5p. *Glia*. (2024) 72:692–707. doi: 10.1002/glia.24497

Any alternative text (alt text) provided alongside figures in this article has been generated by Frontiers with the support of artificial intelligence and reasonable efforts have been made to ensure accuracy, including review by the authors wherever possible. If you identify any issues, please contact us.

Publisher's note

All claims expressed in this article are solely those of the authors and do not necessarily represent those of their affiliated organizations, or those of the publisher, the editors and the reviewers. Any product that may be evaluated in this article, or claim that may be made by its manufacturer, is not guaranteed or endorsed by the publisher.

Supplementary material

The Supplementary material for this article can be found online at: https://www.frontiersin.org/articles/10.3389/fmed.2025.1660291/full#supplementary-material

- 14. Liang G, Meng W, Huang X, Zhu W, Yin C, Wang C, et al. miR-196b-5p-mediated downregulation of TSPAN12 and GATA6 promotes tumor progression in non-small cell lung cancer. *Proc Natl Acad Sci USA*. (2020) 117:4347–57. doi: 10.1073/pnas.1917531117
- $15.\,\mathrm{Tan}$ X, Tong L, Li L, Xu J, Xie S, Ji L, et al. Loss of Smad4 promotes aggressive lung cancer metastasis by de-repression of PAK3 via miRNA regulation. Nat Commun. (2021) 12:4853. doi: $10.1038/\mathrm{s}41467-021-24898-9$
- 16. Fu B, Lin X, Tan S, Zhang R, Xue W, Zhang H, et al. MiR-342 controls *Mycobacterium tuberculosis* susceptibility by modulating inflammation and cell death. *EMBO Rep.* (2021) 22:e52252. doi: 10.15252/embr.202052252
- 17. Zonghai C, Tao L, Pengjiao M, Liang G, Rongchuan Z, Xinyan W, et al. *Mycobacterium tuberculosis* ESAT6 modulates host innate immunity by downregulating miR-222-3p target PTEN. *Biochim Biophys Acta Mol basis Dis.* (2022) 1868:166292. doi: 10.1016/j.bbadis.2021.166292
- 18. Keller A, Leidinger P, Bauer A, Elsharawy A, Haas J, Backes C, et al. Toward the blood-borne miRNome of human diseases. *Nat Methods.* (2011) 8:841–3. doi: 10.1038/nmeth.1682
- 19. Keller A, Leidinger P, Vogel B, Backes C, ElSharawy A, Galata V, et al. miRNAs can be generally associated with human pathologies as exemplified for miR-144. *BMC Med*. (2014) 12:224. doi: 10.1186/s12916-014-0224-0
- 20. Chen L, Liu C, Liang T, Ye Z, Huang S, Chen J, et al. Monocyte-to-lymphocyte ratio was an independent factor of the severity of spinal tuberculosis. *Oxidative Med Cell Longev*. (2022) 2022:7340330. doi: 10.1155/2022/7340330
- 21. Wang Y, Sun Q, Zhang Y, Li X, Liang Q, Guo R, et al. Systemic immune dysregulation in severe tuberculosis patients revealed by a single-cell transcriptome atlas. *J Infect.* (2023) 86:421–38. doi: 10.1016/j.jinf.2023.03.020
- 22. Ashenafi S, Bekele A, Aseffa G, Amogne W, Kassa E, Aderaye G, et al. Anemia is a strong predictor of wasting, disease severity, and progression, in clinical tuberculosis (TB). *Nutrients*. (2022) 14:3318. doi: 10.3390/nu14163318
- 23. Schulman H, Niward K, Abate E, Idh J, Axenram P, Bornefall A, et al. Sedimentation rate and suPAR in relation to disease activity and mortality in patients with tuberculosis. *Int J Tuberc Lung Dis.* (2019) 23:1155–61. doi: 10.5588/ijtld.18.0634
- 24. Sigal GB, Segal MR, Mathew A, Jarlsberg L, Wang M, Barbero S, et al. Biomarkers of tuberculosis severity and treatment effect: a directed screen of 70 host markers in a randomized clinical trial. *EBioMedicine*. (2017) 25:112–21. doi: 10.1016/j.ebiom.2017.10.018
- 25. Wang I., Ding W, Mo Y, Shi D, Zhang S, Zhong I., et al. Distinguishing nontuberculous mycobacteria from *Mycobacterium tuberculosis* lung disease from CT images using a deep learning framework. *Eur J Nucl Med Mol Imaging.* (2021) 48:4293–306. doi: 10.1007/s00259-021-05432-x
- 26. Croker BA, Kiu H, Nicholson SE. SOCS regulation of the JAK/STAT signalling pathway. Semin Cell Dev Biol. (2008) 19:414–22. doi: 10.1016/j.semcdb.2008.07.010

- 27. Xue X, Fei X, Hou W, Zhang Y, Liu L, Hu R. miR-342-3p suppresses cell proliferation and migration by targeting AGR2 in non-small cell lung cancer. *Cancer Lett.* (2018) 412:170–8. doi: 10.1016/j.canlet.2017.10.024
- 28. Cui Z, Zhao Y. microRNA-342-3p targets FOXQ1 to suppress the aggressive phenotype of nasopharyngeal carcinoma cells. *BMC Cancer*. (2019) 19:104. doi: 10.1186/s12885-018-5225-5
- 29. Tian X, Liu Y, Wang H, Zhang J, Xie L, Huo Y, et al. The role of miR-199b-3p in regulating Nrf2 pathway by dihydromyricetin to alleviate septic acute kidney injury. Free Radic Res. (2021) 55:842-52. doi: 10.1080/10715762.2021.1962008
- 30. Petrillo S, Gallo MG, Santoro A, Brugaletta R, Nijhawan P, Russo C, et al. Personalized profiles of antioxidant signaling pathway in patients with tuberculosis. *J Microbiol Immunol Infect.* (2022) 55:405–12. doi: 10.1016/j.jmii. 2021.07.004
- 31. Liu X, Wang X, Chai B, Wu Z, Gu Z, Zou H, et al. miR-199a-3p/5p regulate tumorgenesis via targeting Rheb in non-small cell lung cancer. *Int J Biol Sci.* (2022) 18:4187-202. doi: 10.7150/ijbs.70312

- 32. Leng S, Zheng J, Jin Y, Zhang H, Zhu Y, Wu J, et al. Plasma cell-free DNA level and its integrity as biomarkers to distinguish non-small cell lung cancer from tuberculosis. *Clin Chim Acta.* (2017) 477:160–5. doi: 10.1016/j.cca.2017.11.003
- 33. Jabeen S, Ahmed N, Rashid F, Lal N, Kong F, Fu Y, et al. Circular RNAs in tuberculosis and lung cancer. *Clin Chim Acta*. (2024) 561:119810. doi: 10.1016/j.cca.2024.119810
- 34. Jia H, Zhang L, Wang B. The value of combination analysis of tumor biomarkers for early differentiating diagnosis of lung cancer and pulmonary tuberculosis. *Ann Clin Lab Sci.* (2019) 49:645–9. Available online at: https://www.annclinlabsci.org/content/49/5/645.long
- 35. Matias-Garcia PR, Wilson R, Mussack V, Reischl E, Waldenberger M, Gieger C, et al. Impact of long-term storage and freeze-thawing on eight circulating microRNAs in plasma samples. *PLoS One*. (2020) 15:e0227648. doi: 10.1371/journal.pone.0227648
- 36. Yamada A, Cox MA, Gaffney KA, Moreland A, Boland CR, Goel A. Technical factors involved in the measurement of circulating microRNA biomarkers for the detection of colorectal neoplasia. *PLoS One.* (2014) 9:e112481. doi: 10.1371/journal.pone.0112481